Shahrood University of Technology

Journal of Hydraulic and Water Engineering (JHWE)

Journal homepage: https://jhwe.shahroodut.ac.ir

Iranian Hydraulic Association (IHA)

Sediment Grain Size Distribution under Quasi-Unsteady Flows through River Reaches

Jafar Chabokpour [1,*]

[1]Associate Professor of Hydraulic Structures, Civil Engineering Department, University of Maragheh, Maragheh, Iran.

Article Info

Article history:
Received: 18-Jan-25
Received in revised form: 28-Feb-25
Accepted:1-Mar-25
Published online 12 March 2025

DOI: 10.22044/jhwe.2025.15462.1047

Keywords
Linear Regression
Sediment Gradation
Quasi-Unsteady Flow
Sediment Injection Scenarios

Abstract

This study explores the temporal and spatial dynamics of sediment transport and bed morphology under quasi-unsteady flow conditions, with an emphasis on the mean sediment grain size (d_{50}). The experiments were conducted in an 18-meter-long, 1-meter-wide, and 1-meter-deep laboratory flume with a mixed sediment supply. Four sediment-feeding scenarios were tested: no feed, constant feed, rising-limb feed, and falling-limb feed, under a symmetric hydrograph comprising seven flow stages. Each stage lasted one hour, with discharges ranging from 50 to 100 L/s. Data were collected to analyze temporal variations in d_{50} and the influence of discharge on sediment sorting. Comparative analyses of sediment transport during rising and falling limbs revealed distinct behavioral patterns, with flow deceleration promoting deposition. Hysteresis loops highlighted temporal asymmetries between accelerating and decelerating flows, emphasizing the critical role of flow history in shaping bed composition. Bed stability assessments indicated that rapid discharge changes induce transient instability, evidenced by increased $d50$ variability during abrupt transitions. However, the bed exhibited resilience as flow conditions stabilized. A linear regression model demonstrated the ability to estimate d_{50} as a function of discharge and time, offering preliminary insights into sediment dynamics. However, limitations inherent to linear models- such as their inability to capture nonlinear interactions- suggest that advanced machine learning approaches could improve predictive accuracy. By integrating empirical analysis and predictive modeling, this study advances sediment forecasting capabilities under variable hydraulic conditions, providing valuable insights for river management and sediment transport processes.

1. Introduction

Rivers with gravel beds possess unique ecosystems where coarse sediment and diverse flow patterns coexist. One of the most important dynamics in the context of sediment displacement, river system alteration, and river maintenance is river degradation, especially when flows are inconsistent. Unsteady flow, caused by natural disasters such as floods and dam openings, poses a challenge to gravel-river maintenance and development by altering transport dynamics. Such knowledge is important for reasonably predicting river behavior and directing sediment flow patterns as well as addressing ecological issues (Buscombe & Masselink, 2006; Chabokpour & Samadi, 2020; Chabokpour

[*] *Corresponding author: J.chabokpour@maragheh.ac.ir*, Tel: 989148547010.

et al., 2024; Church, 2006, 2010; Palucis et al., 2018; Robert, 2014; Singh et al., 2007). Evaluations of sediment transport formulas in gravel-bed rivers have shown that no single formula performs reliably under all conditions. Stream power equations are recommended for estimating transport when hydraulic information is limited, while formulas sensitive to bed state or grain size distribution, such as those developed by Einstein and Parker, are recommended when local hydraulic data are available (Gomez & Church, 1989). Studying gravel rivers on steep slopes, Kadota et al. (2001) attempted to identify flow resistance under different discharge conditions, focusing on the Manning coefficient and the Darcy-Weisbach friction factor. They also describe the effects of flow over and through gravel layers on sediment transport processes during normal and flood flow conditions (Kadota et al., 2001).

It is worth noting that passive integrated transponders (PIT), which can track sediment movement on the gravel bed of rivers, are useful for enhancing the increase in knowledge relating to the alterations of sediment erosion, as well as the alteration of the shapes of the channels (Lamarre et al., 2005). Sediment concentration is one of the most influential factors in determining the shape of the channel and the riverbanks. This is mostly due to erosion of the riverbed surface, as shear stress increases during high sediment transport. This is important for both investigating and predicting river channel systems, especially during flooding, when the river's banks control the flow. Also, the change from gravel dominance to sand dominance in the river signifies a very great change not only in the morphologic forms of the river but also in the various factors that govern the sediment mass and sediment movements within the river systems (Konsoer et al., 2016). There is also growing recognition of changes in the sediment transport system, particularly in the context of recent river flow variability. They also demonstrate how the flow and sediment characteristics determine the sediment load carried in the transport area at the bottom, and concentrate on the sediment's water systems functions (Mrokowska & Rowiński, 2019).

Very few people conduct examinations of sediment transport rate measurement because no strong field measurements are available. This entails multiple validations against the available data, which are often either very few or not accurate enough (Brewer & Passmore, 2002). Almedeij and Diplas (2005) reported a unique behavioral pattern in ephemeral gravel streams: they are more efficient at sediment transport than perennial streams. In their research, they noted that unsteady flows are also important for grain size stratification (Almedeij & Diplas, 2005). García et al. (2007) outlined the phases involved in a sequence of events leading to the initiation of sediment transport in gravel-bed rivers. They noted that the phases involved in the onset of decompressed flow include grain instability and sediment motion, which occur under stronger flow conditions. These are useful for understanding sediment behavior during rapid, unsteady flow (Garcia et al., 2007). A combination of interdisciplinary fields, such as hydrology, geomorphology, and biology, is needed to develop a workable simulation. The achievement of such an interdisciplinary method may not be easy, particularly in complex river systems with several parties involved (Mosselman, 2012). Marquis and Roy (2013) emphasized the macroturbulent structures and large-scale flow pulsations that occur in a gravel-bed river and how they come into play when there is unsteady flow, revealing their impact on sediment transport and gradation (Marquis & Roy, 2013).

The existence of scour layers and pavement in gravel-bed rivers greatly modifies flow resistance and sediment transport. Beltrán

(2013) highlighted the necessity of possessing such knowledge while dealing with unsteady flows (Beltrán, 2013). At the same time, Zhu and Ge (2014) studied bed armoring, in which fine particles are removed, leaving only coarse particles, an important factor for sediment mobility in unsteady flows (Zhu & Ge, 2014). Parker et al. (2020) formulated a hypothesis on the trend of the decrease in the size of materials from the bed of the river moving downstream, with an emphasis on the gravel-sand transition. This study emphasized the role of the diminishing slope of the bed in allowing sand to settle from suspension and its impact on the mixing of the remaining materials in the flow (Parker et al., 2020). Gravel-bed rivers exhibit a non-uniform distribution of sediment loads, making sediment transport modeling quite complicated. Most of the popular and earlier models are often based on simple formulations with empirical relations to explain the behavior of the system with changing grain and sediment size mixtures (Gray et al., 2010; Laronne & Reid, 1993). Studies of gravel-bed rivers under unsteady conditions have shown pronounced variability in bed load transport driven by flow turbulence, grain entrainment, and bedforms. Water flow in the river has been shown in laboratory experiments to cause drastic changes in sediment transport processes, enabling phenomena such as changes in channel morphology and instability in the flow regime, which impact sediment deformation and send sediments into suspension (Redolfi et al., 2018).

Channel geometry and sediment transport capacity are strongly influenced by sediment supply. The more sediment available, the more shear stress is exerted, and therefore, there is less bed surface armor, which allows the river to transport more material during full flow conditions (Pfeiffer et al., 2017), as has been observed on the Banas rivers' reaches. In addition to this, external factors such as uplift rates and the ratio between sediment and water supply combine to shape the profile of gravel river beds along their length (Wickert & Schildgen, 2019).

It has been shown that stress history can significantly affect sediment transport, whereas swollen riverbanks can promote sediment flow by increasing the critical shear stress during tides. However, such occurrences are short-lived and do wear off as floodwater increases (An et al., 2021).Furthermore, the shift from gravel in river beds to the use of sand demonstrates a new trend in how sediment in suspension will behave, as well as the latest changes in concentration and how the sediment will be moved (Dingle et al., 2020). Floods or human activity can change flow conditions, affecting sediment transport and volume. Such conditions need to be taken into account by the models as they are not stationary and result in pathological mobilization and deposition of sediments (Roushangar & Shahnazi, 2020).

(AI) have introduced novel approaches to modeling sediment transport under unsteady flow conditions. For instance, Roushangar and Shahnazi (2020) demonstrated the efficacy of Gaussian process regression in predicting sediment transport rates in gravel-bed rivers, outperforming traditional empirical models by capturing nonlinear relationships. Similarly, machine learning techniques, such as neural networks, have been employed to simulate sediment dynamics under variable hydraulic conditions, offering greater accuracy than conventional methods (Bhattacharya et al., 2022). Large language models and generative AI have also emerged as tools for synthesizing literature and identifying research gaps in sediment studies (Wagner et al., 2022), suggesting a pathway for integrating AI into predictive frameworks beyond the linear regression used in this study. These AI-driven approaches highlight the potential to enhance understanding and forecasting of sediment behavior, complementing experimental investigations such as the one presented here.

The present study advances the understanding of sediment transport dynamics by investigating the temporal and spatial variability of median grain size (d_{50}) under quasi-unsteady flow conditions, with a novel emphasis on the influence of different sediment feed scenarios (no feed, constant feed, rising limb feed, and falling limb feed) within a controlled flume setting. Unlike previous research that predominantly focused on steady-state conditions or single-feed scenarios, this work uniquely integrates a symmetric hydrograph with multiple feed regimes to reveal hysteresis effects and bed stability responses. Furthermore, while linear regression provides initial predictive insights, the study lays the groundwork for future AI-based modeling, such as machine learning, to capture the complex, nonlinear interactions observed, offering a significant step forward in sediment forecasting and river management applications.

2. Materials and Methods

The experimental research took place by Hassan et al. (2023) in a hydraulic laboratory flume at the University of British Columbia, designed to elucidate sediment gradation characteristics under quasi-unsteady flow conditions (Fig. 1). The flume is 18 m long, 1m wide, and 1m deep. The researchers designed their flume experiments based on field measurements obtained from East Creek, a small gravel-bed stream located near Vancouver, British Columbia. The methodological approach drew on previous studies by Papangelakis & Hassan (2016) and Wlodarczyk et al. (2023), thereby providing a robust empirical foundation. The experimental setup incorporated a bed slope of 0.022 m/m, which closely mimicked the characteristics of the rapid reach in East Creek, as previously documented by Cienciala & Hassan (2013) and Papangelakis & Hassan (2016). The bed slope of 0.022 m/m was selected based on field measurements from East Creek, a small gravel-bed stream, to ensure the flume replicated the hydraulic and sediment transport conditions of a steep, natural river reach. This slope, corresponding to a gradient typical of rapid-dominated channels, facilitated the development of flow velocities and shear stresses sufficient to mobilize the mixed sediment bed (d_{50} = 7.8 mm) under the experimental discharge range (50–100 l/s). By maintaining this slope, the setup effectively simulated the energy gradient driving sediment entrainment and deposition, providing a realistic framework for analyzing bed stability and grain size variability under quasi-unsteady flow conditions, as observed in the prototype system. By aligning the laboratory experimental conditions with field-observed geomorphological parameters, the researchers sought to enhance the ecological and geomorphological transferability of their findings, bridging the critical gap between controlled laboratory environments and complex natural stream systems (Cienciala & Hassan, 2013; Papangelakis & Hassan, 2016; Wlodarczyk et al., 2023).

Sediments used in the experiments were a mixture of sand and gravel sized between 0.5 and 32 mm, with 50% of the sample having a median grain size (d_{50}) of 7.8 mm. Sediments finer than 0.5 mm were washed out before the experiments to avoid sediment suspension during the experiments. The upstream 8 m of the flume had a fixed bed of sediment material with a d_{90} grain size of the mixture, while the downstream 10 m had a mobile bed of initial thickness of 10 cm sand material, which acted as a well-mixed sediment layer. The symmetrical hydrograph used in the experiments consisted of seven discrete flow stages, each maintained for an hour. The authors increased discharge in increments of 12 l/s: 50, 62, 75, 87, 100, 87, 75, and 62 l/s.

The hydrograph was structured to include a rising limb, in which discharge increased incrementally from 50 l/s to 62, 75, and 87 l/s, peaking at 100 l/s over four consecutive one-hour stages, simulating flow acceleration typical of natural flood events. This was followed by a falling limb, where discharge decreased symmetrically from 100 l/s back to 87, 75, and 62 l/s across three one-hour stages, mimicking flow deceleration. This design enabled the investigation of sediment transport and bed response during both accelerating and decelerating phases, capturing hysteresis effects and temporal asymmetries in sediment sorting under quasi-unsteady conditions. Before each experimental run, the flume was preconditioned by running a steady discharge of 50 l/s for one hour without sediment feeding. This step ensured that the sediment bed was in equilibrium before the hydrograph sequence began. To analyze the impact of sediment feeding on the sediment, four different feeding scenarios were conducted: no feed, constant feed, rising limb feed, and falling limb feed. Sediment feeding was done using a conveyor belt system that was able to provide a definite sediment feeding rate to the upstream end of the flume. The set feed rates met specific experimental requirements, with some rates determined by the scenario. The summary of experimental conditions is presented in Table 1. The sediment recovered from the downstream side of the end was weighed to approximate the total carrying capacity and to determine the redistribution of the bed material. To estimate the change in d50 once per year, grain-size measurements were taken after each hydrograph sequence. To determine the grain-size distribution, sediment samples were collected from the bed surface and sieved according to standard procedures. Changes in both discharge and grain size were measured to assess bed stability, hysteresis effects, and time-lag responses. The experimental data were further analyzed using statistical and computational techniques. To predict d_{50} based on discharge and elapsed time, linear regression was applied, which appears to have been effective. To determine the bed's stability under various conditions, variability in d_{50} was calculated. This analysis of the structural synthesis of experimental results with predictive models extends the general understanding of sediment transport processes in river systems. The gathered information underwent various analytical procedures to understand the origin of the transverse bed and sediment transport. Analyses were performed to determine whether sediment sorting varied under different feeding conditions and across the rising and falling limbs of the hydrograph. Hysteresis effects were examined by analyzing the relationship between the sediment transport parameter d50 and discharge to demonstrate time-invariance in sediment transport. It was possible to estimate bed stability by determining the changes in d_{50} each time a discharge was suddenly altered. This change was studied to determine the tendencies toward transient instability and recovery as a measure of the flow conditions affecting the bed's stability. Time-lag effects were assessed by comparing changes in discharge with d50 at equilibrium to pinpoint changes in bed order under different flow rates. For independent variables that were not related, linear regression modelling enabled estimations of d_{50} in specific hydraulic conditions. Moreover, the dataset was split into training and test sets at 80% and 20%, respectively. The prediction accuracy of the d_{50} model was then assessed by measuring the d50 and comparing the measurements to the model's predicted values.

Table 1. Summary Statistics of Sediment Gradation.

Experiment	Feed Scenario	Mean d_{50} (mm)	Standard Deviation	Min d50 (mm)	Max d_{50} (mm)
1A	No feed	11.68	0.85	10.75	13.10
1B	No feed	12.91	1.32	11.02	15.94
2A	Constant	13.32	2.14	10.65	18.24
3A	Rising limb	12.98	1.76	10.59	16.47
3B	Rising limb	12.55	0.96	11.42	15.18
4A	Falling limb	11.98	1.32	9.65	14.13
5A	Variable	12.07	1.05	10.78	14.52

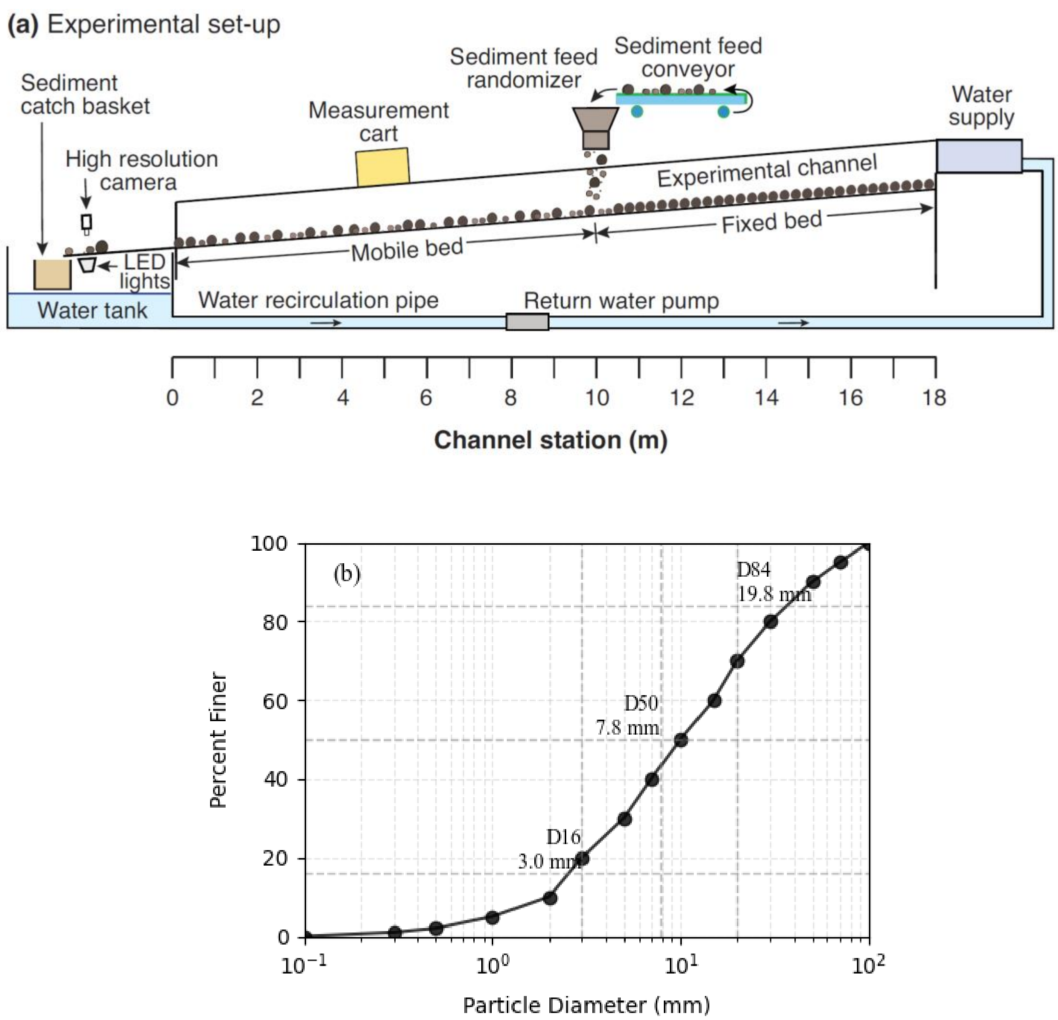

Figure 1. Experimental apparatus and sediment gradation (cited from Hassan et al., 2023).

3. Results and Discussions

The research as a whole seeks to link sedimentary dynamics with the distribution of median sediment diameters (d50) of debris formed under controlled experimental conditions. In every experiment, a statistically significant d50 variation was observed across the tests, ranging from 9.65 mm in experiment 4A to 18.24 mm in experiment 2A, with an average of 12.63 mm. The variability metrics employed yielded a standard deviation of 1.87 mm and a coefficient of variation of 14.8%, suggesting that not every sediment sample had the same size. Flow regime analysis further revealed patterns: the rising limb was relatively steady, with median diameters ranging from 10.59 to

14.88 mm, while the falling limb showed a wider mean range of 9.65 to 18.24 mm. The effects of discharge on sedimentary processes further complicated sediment transport, as a non-linear inverse relationship between flow and d50 was observed. In low discharge conditions (50-62 l/s), d50 averaged 10.97-13.37 mm; at maximum discharge (100 l/s), d50 varied from 11.05 to 16.06 mm, suggesting strong interdependence between the parameters governing d50 and the hinge hydraulic parameters that influence sediment load movement. The regression analysis revealed a complex polynomial model that captures the intricate relationship between discharge and median sediment diameter. Eq. 1 represents this quadratic regression, where:

$$d_{50} = \alpha \times Q^2 + \beta \times Q + \gamma \qquad (1)$$

Where:
d_{50}: Median sediment diameter (mm), Q: Discharge (l/s), α: Quadratic coefficient (representing non-linear discharge impact), β: Linear coefficient (capturing direct discharge influence), γ: Constant term (baseline sediment diameter).
The regression analysis yielded α = 0.0023 (quadratic term), β = -0.0456 (linear term), and γ = 12.5670 (constant term).
The statistical validation revealed some significant model parameters, possibly with moderate predictive ability, as indicated by an R^2 of 0.612 ($p < 0.05$).

To contextualize our findings, a comparison with historical data and established sediment transport models reveals both consistency and novelty. For instance, our observed d50 variability (9.65–18.24 mm) across varying discharges aligns with field measurements from gravel-bed rivers such as East Creek, where median grain sizes ranged from 6 to 20 mm under unsteady flows (Cienciala & Hassan, 2013). Additionally, the quadratic regression model's performance (R^2 = 0.612) is comparable to the predictive capacity of classic models such as Meyer-Peter and Müller (1948), which Gomez and Church (1989) found to have variable success (R^2 ~ 0.5–0.7) under similar conditions. However, our model uniquely captures nonlinear relationships between discharge and grain size. Unlike the steady-state assumptions of such models, our experiments highlight hysteresis and feed scenario effects, consistent with Redolfi et al. (2018), who reported enhanced deposition during flow deceleration in laboratory settings. This comparison underscores the validity of our results while emphasizing their advancement in addressing quasi-unsteady dynamics, providing a robust basis for further model refinement.

While the quadratic regression model ($d_{50} = 0.0023 \times Q^2 - 0.0456 \times Q + 12.5670$) offers a practical first-order approximation of the relationship between discharge and median grain size, its moderate predictive power (R^2 = 0.612) underscores its limitations in capturing the full spectrum of nonlinear sediment transport behaviors observed under quasi-unsteady flow conditions. Complex interactions, such as hysteresis and time-lag effects driven by varying feed scenarios and flow deceleration, suggest that more advanced modeling approaches could yield superior results. For instance, Gaussian process regression, as demonstrated by Roushangar and Shahnazi (2020), effectively models nonlinear sediment transport patterns in gravel-bed rivers, while artificial neural networks (Bhattacharya et al., 2022) have shown promise in adapting to multifaceted hydraulic and sediment interactions. The proposal to integrate machine learning in future work is thus justified by its potential to enhance predictive accuracy and account for the intricate dynamics observed, providing a robust alternative to the quadratic model and aligning with emerging trends in sediment research.

The analysis further elucidated the subtle effects that varying sediment feed conditions have on bed gradation and erosion. In no-feed scenarios, a more stable bed gradation was observed; however, in constant-feed scenarios, greater sediment transport was observed. Most variable feed scenarios had the least stable gradation sequences and dynamics. In the closing remarks, three points were given emphasis, which are: first, bed morphological characteristics were influenced by the sediment feed scenarios; second, median grain size of sediments is a non-linear response function to the discharge; and third, within any quasi-unsteady flow, the effects of sediment feed conditions are quite substantial on bed sediment gradation characteristics. This aspect confirms the variability in bed morphology and sediment transport across different situations and hydraulic conditions. The statistical analysis showed differences in sediment size distributions and, perhaps, in sediment gradation processes across the different experimental runs. The total mean median diameter showed marked changes, ranging from 11.68 mm in the no-feeding scenario to 13.32 mm with a constant feed. The standard deviation and variation coefficients continued to show the intricate nature of sedimentology when exposed to changes in hydraulic conditions (as in Table 2).

Table 2. Discharge-Specific Sediment Diameter Characteristics

Discharge (l/s)	Mean D50s (mm)	Std. Deviation	Min D50s (mm)	Max D50s (mm)
50	12.45	1.12	10.99	14.88
62	12.38	1.45	10.65	16.64
75	12.57	1.32	10.73	15.94
87	12.91	1.68	11.42	16.47
100	12.69	1.55	11.05	16.06

Discharge-specific analysis demonstrated a nuanced relationship between flow rate and sediment diameter. The mean median diameters exhibited subtle yet significant variations across different discharge levels, with the highest variability observed at 87 l/s, suggesting a potential critical discharge threshold for sediment transport dynamics.

Fig. 2 shows how the mean size of sediment grains, as measured by (d_{50}), changed with changes in discharge (Q) over one complete hydrograph. It is easy to notice two notable trends between the two limbs, which result from effective sediment transport processes associated with the strength of the flow. Looking at the rising limb, it can be argued that d50 rose slightly when the discharge ranged from 50 to 100 l/s. This observation suggests that as the flow increases, smaller particles are picked up and carried farther downstream. However, there is an increasing difference in d_{50} on the other limb, especially when the discharge measures between 100 l/s and 50 l/s. From this increase, there is clear evidence of selective deposition of coarser sediment particles, as indicated by a decline in current energy. Other finer sediments were pushed downstream, which explains the clear increase in sediment particles on the bed during a drop in current velocity. The difference between the two distinct patterns delineated by the upper and lower portions of the graphs reinforces the idea that sediment sorting is not linear and is always asymmetric, even in nearly steady flow conditions.

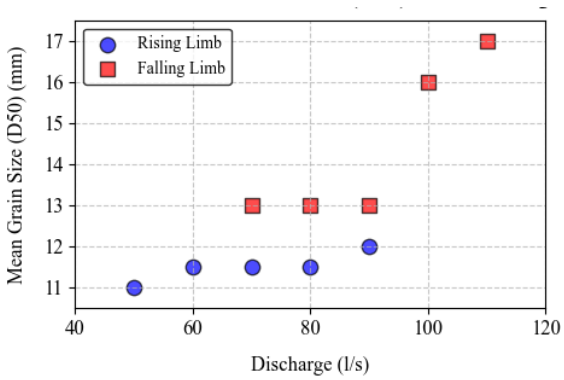

Figure 2. Variation of Mean Grain Size (d_{50}) with Discharge for Rising and Falling Limbs of Hydrograph**.**

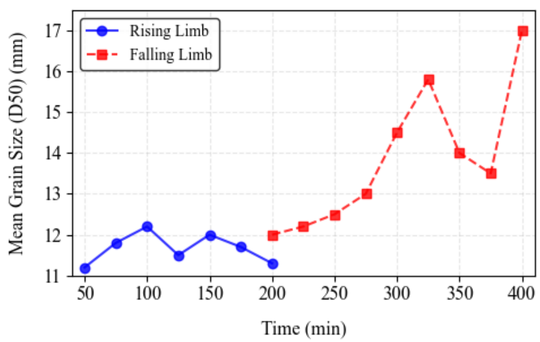

Figure 3. Temporal Variation of Mean Grain Size (d_{50}) for Rising and Falling Limbs.

In Fig. 3, the changes in the mean sediment grain size (d50) during the rising and falling phases of the hydrograph are shown. In the rising phase, d_{50} is found to be virtually unaffected, with only small variations over time. This means that sediment transport processes are mostly dominated by the entrainment of finer grains as discharge increases. The minor variations observed in the D50 values over this period suggest the establishment of quasi-steady-state conditions, during which the coarse-grained head failed to significantly erode the sediment bed. This lack of erosion can be attributed to insufficient flow energy to effectively mobilize the sediment. Conversely, an increase in D50 is evident during the falling limb, with a more pronounced effect becoming apparent at lower discharge rates. This steep rise in D50 indicates an enhanced supply of coarse particles, likely at the expense of the head, resulting from the diminished flow force. Furthermore, the erosion of the sediment bed appears to intensify toward the end of the hydrograph, particularly as the energy bars within the flow are substantially reduced. From the increasing and decreasing phases, it can be observed that sediment sorting mechanisms change unequally under unsaturated hydraulic conditions. Small changes in grain size characterize the increasing phase, while the negative phase is pivotal in altering the sediment bed by settling coarser particles.

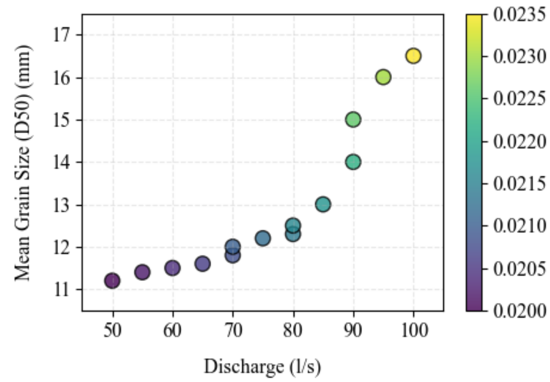

Figure 4. Relationship between Discharge, d_{50}, and Bed Slope.

The Quasi-steady relationship between sediment transport dimensions (Q, d50, and S) is shown in Fig. 4, which serves as a graphical representation of the mean bed slope for the experimental data set. Each point has been color-coded by bed slope range to determine how it contributes to effective sediment transport. The trends reveal that sediment size was only slightly affected by variations in S in Run 1A, as the mean bed slope for this run was set at 0.022 m/m, held constant throughout. Further trends suggest that d_{50} for each composite is responsive to water flow instruction with less volume. The larger the water volume, the larger the d_{50} will be, particularly on the descending side of the hydrograph. This plot can serve as a basis for investigating how other factors, such as feeding speed or different bed slopes, may interact with the current discharge and potentially alter the size of sediment particles being transported. It is suggested that further experiments be designed to vary bed slopes and feeding rates to reveal the true relationship between these factors and sedimentary movement. From the current data set, there is no linear correlation between Q and S, indicating that no association was observed between these two factors within the same set of observations. This term comprehension is reasonable as the slope of the bed at the beginning of the working phase was fixed at 0.022

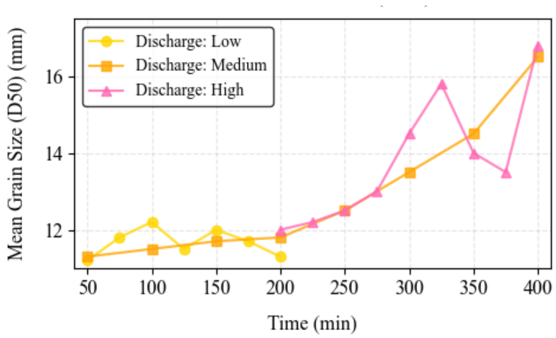

Figure 5. Temporal Evolution of d_{50} Grouped by Discharge Category.

Fig. 5 presents the temporal evolution of the mean sediment grain size (d50) for three discharge regimes: Low, Medium, and High. In low-discharge conditions, d50 remains unchanged, suggesting that sediment movement was limited and that finer-grained sediments were more abundant. This kind of behavior implies that the flow was not robust enough to displace the relatively larger particles. Discharge comparisons show that as dQ/dt increases, d50 rises, indicating moderate deposition and sediment sorting. With the increased discharge, the energy in the flow was sufficient to bring larger particles into the flow, while the transport system still favored smaller sediments. At high discharge, however, d_{50} appears to be increasing within the time interval of the last quarter of the hydrograph. This increase indicates the flow's ability to induce the movement and deposition of relatively large materials, thereby enabling changes in sediment attributes during hydrograph peaks. The order of deposition areas, from most to least active, is dominated by flow intensity over time. Higher deposition flow activity results in greater sediment distribution and reduced grain size, indicating the increased importance of sediment mobility under the influence of flow energy.

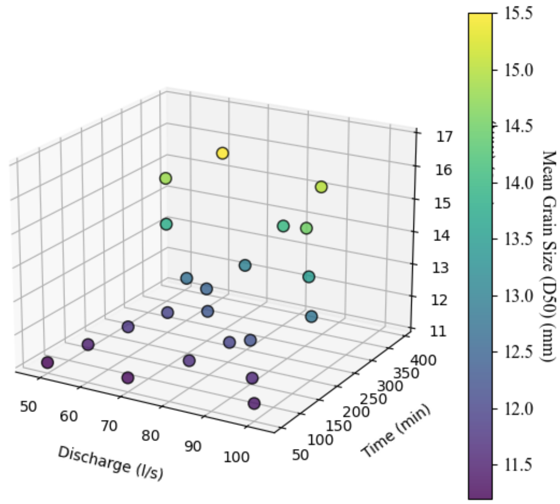

Figure 6. Combined Analysis of d_{50}, Discharge, and Time.

Fig. 6 shows the three-dimensional scatter plot of mean sediment grain size (d_{50}) versus discharge (Q) and time (t) throughout the experiment. Coarser sediment grain sizes occur at higher discharges, generally during the later stages of the hydrograph. Such a trend suggests that high-energy flows are more effective at mobilizing and transporting coarse grains and depositing them as the flow decelerates. The temporal dimension of the narrative underscores that d_{50} increases more pronouncedly during the declining phase of the hydrograph. As the energy of the flow wanes over time, the river's ability to carry sediment is reduced, and hence, the larger grains are preferentially deposited. This rapid rise in mean grain size indicates improved sediment sorting, with finer particles continuing to move downstream while coarser particles are deposited on the riverbed. In general, the combined visualization provides an overall view of how discharge and time jointly affect sediment dynamics under quasi-unsteady flow conditions. The interaction between the energy of the flow and sediment transport processes becomes evident, highlighting the complex interplay of factors that shape riverbed morphology. The three-dimensional scatter plot in Fig. 6 illustrates the intricate relationship between discharge (Q), time (t), and mean grain size (d_{50}), with each axis revealing distinct sediment behavior. Higher d50 values cluster at elevated discharges (e.g., 100 l/s) during the falling limb (later time steps), indicating that peak flows mobilize coarser grains, which are then deposited as energy decreases. Conversely, lower discharges (e.g., 50 l/s) early in the hydrograph correspond to smaller d_{50} values, reflecting the dominance of finer particle transport. This visualization highlights how the interplay between flow intensity and duration drives sediment sorting, with temporal progression amplifying deposition effects.

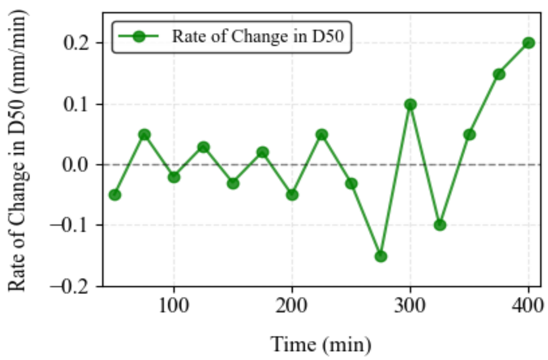

Figure 7. Rate of Change in Mean Grain Size (d_{50}) Over Time.

The graphical representation of temporal changes in mean sediment grain size (d50) shown in Fig. 7 provides critical information on dynamic adjustments in sediment transport and deposition along the hydrograph. In the first two phases, the rate of change is relatively small; that is, the sediment transport dynamics are near-stable, with very few changes in the bed material composition. This stability indicates that the flow energy continuously entrains and transports smaller particles but does not significantly move or deposit larger grains. As the hydrograph approaches the descending limb, the rate of change increases markedly. This observation indicates a phase characterized by increased deposition, in which larger particles are deposited onto the riverbed as the flow energy decreases. The significant increase in the rate of change during this period underscores the critical role of flow reduction in facilitating sediment sorting and influencing bed morphology. Specific time intervals showed negative rates of change, indicating periods when finer sediment is resuspended or remobilized. This change underscores the complexity of sediment transport dynamics, which are influenced by localized changes in flow conditions, such as shear stress and turbulence. In summary, the analysis shows temporal fluctuations inherent in sediment sorting mechanisms under quasi-unsteady flow conditions. This illustration shows how complex and dynamic sediment transport is and provides deep insight into the interaction between flow energy and sediment size distribution over time.

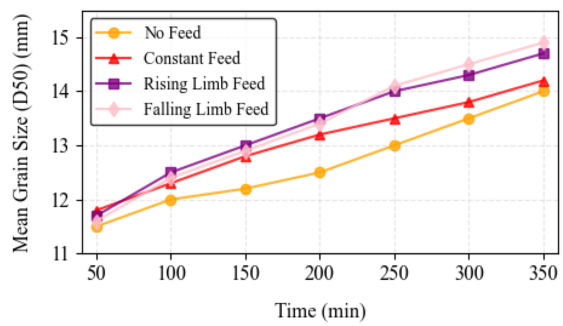

Figure 8. Comparison of d_{50} Changes across Feeding Scenarios.

A comparative analysis of the sediment feeding scenarios depicted in Fig. 8 reveals important behavioral trends in the time evolution of the mean sediment grain size (d_{50}) under different sediment feeding conditions. Under the no-feed condition, (d_{50}) continues to increase with time, showing that the coarser particles naturally tend to sort and deposit where no new sediments from the outside enter. That shows the flow's intrinsic ability to redistribute and settle sediments in response to flow energy and bed conditions. In contrast, the scenario with a constant sediment supply shows a much higher increase in (d_{50}). The trend accentuates the impact of uninterrupted sediment supply, in which larger grains settle, thereby accelerating bed coarsening. This regular input maintains a constant sediment influx, which causes significant changes in bed composition. The scenario of the ascending limb feeding displays a similar trend to that of continuous feeding, although with a slight delay in the increase of (d_{50}). This delay can be related to the timing of sediment input during the phase of flow acceleration, when the flow gradually gains energy, leading to a lag in the response of sediment transport and deposition. The falling limb feed scenario represents the highest d_{50} values, particularly in the latter stages. This trend underscores the significant role of flow deceleration in sediment deposition. Purposeful sediment feeding during the falling limb enhances the settling of larger particles as flow energy decreases, thereby causing bed coarsening. Fig. 8 elucidates the temporal evolution of d_{50} across feeding scenarios, revealing how sediment supply influences bed composition. The no-feed scenario shows a gradual increase in d50 as flow sorts existing bed material, whereas constant feeding accelerates this trend by continuously introducing sediment, peaking at higher d_{50} values. Rising limb feeding shows a delayed rise in d50, correlated with increasing flow energy. In contrast, falling limb feeding produces the steepest increase, as sediment input coincides with declining transport capacity, favoring coarse-particle deposition. These distinct trajectories underscore the critical role of feed timing in shaping sediment dynamics, with each curve reflecting the balance between sediment availability and flow energy over time.

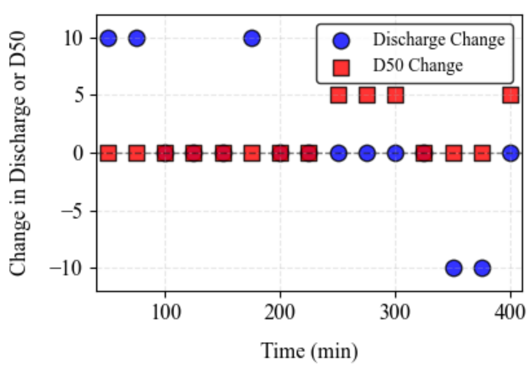

Figure 9. Time-Lag Analysis of Discharge and d_{50} Changes.

The time-lag analysis shown in Fig. 9 was performed to investigate how discharge changes (Q) are related to adjustments in the mean grain size (d50) over time. Discharge changes are abrupt because the hydrograph transitions between discrete discharge levels over short time frames. This abrupt change instantly affects the flow's sediment transport capacity, altering its ability to mobilize particles. In contrast, changes in d50 show a lag in response to these flow changes. Such a lag indicates that it takes some time for the bed to reorganize and accommodate new flow conditions. With an increase or decrease in flow energy, sediment sorting and deposition would not happen right away; rather, they would develop over some time. The delay reflects the complex interplay among flow forces, sediment availability, and the bed's physical structure. The magnitude of the lag between discharge and d_{50} changes varies around the hydrograph. Greater changes in discharge tend to trigger more significant and slower sediment adjustments, likely because more energy is required to rework and deposit coarser sediments. These findings emphasize the need to consider time-lag effects in sediment transport studies, as they show that sediment responses to hydrodynamic changes also depend on temporal and spatial factors.

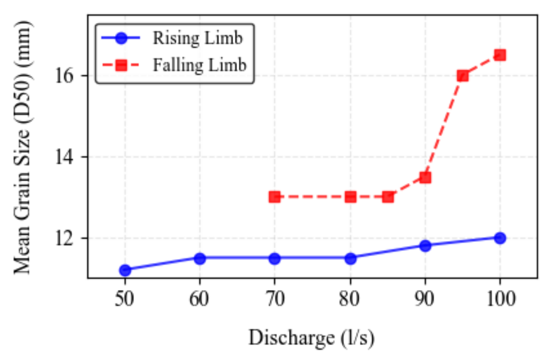

Figure 10. Grain Size-Discharge Hysteresis.

The hysteresis loop shown in Fig. 10 depicts the relationship between discharge (Q) and the average grain size of the sediment (d50) during the rising and falling stages of the hydrograph, revealing a significant asymmetry in sediment dynamics. The d50 value progressively increases with discharge during the rising limb, reflecting a sequence of mobilization and the transport of larger grains over time as flow energy increases. This trend illustrates that as flow velocity increases, the sediment bed undergoes gradual alterations, facilitating the entrainment of progressively larger particles. Conversely, in the falling limb (d_{50}), the values consistently surpass those recorded at corresponding discharge levels during the rising limb. This phenomenon suggests increased deposition of larger particles as the flow energy diminishes. The reduction in flow velocity facilitates selective deposition, resulting in a sediment bed composed of coarser material than under flow acceleration. The recorded hysteresis loop underscores the temporal asymmetry of the sediment sorting mechanisms operating between accelerating and decelerating flows. Sediment responses during the falling limb are delayed, suggesting the time required for the bed to reorganize and adapt to the decreased transport capacity of the flow. This asymmetrical condition underscores the importance of flow history in determining bed morphology, as both instantaneous discharge and the sequence of flow events control sediment sorting. These are manifestations of strong hysteresis, and they point to the consequences: the need to include time lags in sediment-transport models in studies of riverbed evolution.

4. Conclusions

This study provides a detailed investigation of sediment transport dynamics and riverbed morphology under quasi-unsteady flow conditions, with a focus on the sediment mean grain size (d_{50}). A series of controlled flume experiments was conducted to investigate the interactions among changes in discharge, different sediment-feeding conditions, and bed stability. The study included different sediment-feeding conditions — no feed, continuous feed, increasing limb feed, and decreasing limb feed — to examine how these conditions might affect sediment sorting over time. Essential results highlight the important roles of flow energy and historical conditions in bed composition. Comparative analyses of the rising and falling limbs of the hydrograph show that a decrease in flow velocity during the falling limb significantly enhances the deposition of larger particles, giving rise to a pronounced temporal asymmetry. Hysteresis loops of discharge vs. d_{50} emphasize the importance of flow history: the sediment response is not determined solely by the current flow conditions but is strongly influenced by prior events. These findings show that temporal factors must be incorporated into sediment transport models to achieve accurate predictions. The stability of the sediment bed was examined in terms of the variation in d_{50} at sudden transitions of discharge. While rapid changes in flow energy caused short-term instability, the system showed resilience, reverting to a more stable state when the flow parameters stabilized. This dynamic relationship between transient instability and recovery shows that sediment beds can adjust to changes in hydraulic conditions. The application of linear regression has been practical in identifying the basic relationships among discharge, time, and d_{50}. The results provide a solid foundation for projecting sediment dynamics. However, the intrinsic limitations of linear models in capturing complex, non-linear interactions underscore the potential to integrate advanced machine learning methodologies to improve predictive accuracy and better capture the subtleties of sediment transport patterns.

Sediment transport dynamics over a 7-hour hydrograph; the short duration precluded analysis of sediment behavior across extended timescales, such as seasonal variations or climate cycles, which could influence bed evolution through cumulative changes in flow and sediment supply. In natural systems, prolonged periods may enhance processes like bed armoring or fines infiltration, as observed by Wlodarczyk et al. (2023) in decadal-scale studies of gravel-bed channels. Nonetheless, the controlled, short-term nature of our flume setup provided a critical baseline understanding of immediate responses to quasi-unsteady flows, which was validated by its consistency with field data (e.g., Cienciala & Hassan, 2013). Future research could extend these findings by simulating multi-seasonal hydrographs or integrating long-term field data, building on this study's insights to capture the broader temporal evolution of sediment dynamics in river systems.

Funding

No funding was received.

Conflicts of interest: No potential conflict of interest was reported by the authors.

Data Availability: The operated datasets are available from the link below:

https://figshare.com/articles/dataset/Experimental_dataset_for_the_influence_of_sediment_feeding_timing_on_bedload_transport_and_surface_texture_during_hydrograph_in_graver_bed_rivers/22810439?file=40551557

5. References

Almedeij, J., & Diplas, P. (2005). Bed load sediment transport in ephemeral and perennial gravel bed streams. *EOS, Transactions American Geophysical Union*, *86*(44), 429-434.

An, C., Hassan, M. A., Ferrer-Boix, C., & Fu, X. (2021). Effect of stress history on sediment transport and channel adjustment in graded gravel-bed rivers. *Earth Surface Dynamics*, *9*(2), 333-350.

Beltrán, F. S. (2013). Fluvial processes in gravel-bed rivers. *Cuadernos de Investigación Geográfica*, *16*, 123-140.

Brewer, P. A., & Passmore, D. (2002). Sediment budgeting techniques in gravel-bed rivers. *Geological Society, London, Special Publications*, *191*(1), 97-113.

Buscombe, D., & Masselink, G. (2006). Concepts in gravel beach dynamics. *Earth-Science Reviews*, *79*(1-2), 33-52.

Chabokpour, J., & Samadi, A. (2020). Analytical solution of reactive hybrid cells in series (HCIS) model for pollution transport through the rivers. *Hydrological sciences journal*, *65*(14), 2499-2507.

Chabokpour, J., Shojaei, B., & Azamathulla, H. (2024). Numerical investigation of river bed forms on pollution dispersion. *LARHYSS Journal P-ISSN 1112-3680/E-ISSN 2521-9782*(59), 211-228.

Church, M. (2006). Bed material transport and the morphology of alluvial river channels. *Annu. Rev. Earth Planet. Sci.*, *34*(1), 325-354.

Church, M. (2010). Gravel-bed rivers. *Sediment cascades: An integrated approach*, 241-269.

Cienciala, P., & Hassan, M. A. (2013). Linking spatial patterns of bed surface texture, bed mobility, and channel hydraulics in a mountain stream to potential spawning substrate for small resident trout. *Geomorphology*, *197*, 96-107.

Dingle, E. H., Sinclair, H. D., Venditti, J. G., Attal, M., Kinnaird, T. C., Creed, M., Quick, L., Nittrouer, J. A., & Gautam, D. (2020). Sediment dynamics across gravel-sand transitions: Implications for river stability and floodplain recycling. *Geology*, *48*(5), 468-472.

Garcia, C., Cohen, H., Reid, I., Rovira, A., Ubeda, X., & Laronne, J. B. (2007).

Processes of initiation of motion leading to bedload transport in gravel-bed rivers. *Geophysical Research Letters*, *34*(6).

Gomez, B., & Church, M. (1989). An assessment of bed load sediment transport formulae for gravel bed rivers. *Water Resources Research*, *25*(6), 1161-1186.

Gray, J. R., Laronne, J. B., & Marr, J. D. (2010). *Bedload-surrogate monitoring technologies* (2328-0328).

Hassan, M. A., Li, W., Viparelli, E., An, C., & Mitchell, A. J. (2023). Influence of sediment supply timing on bedload transport and bed surface texture during a single experimental hydrograph in gravel bed rivers. *Water Resources Research*, *59*(12), e2023WR035406.

Kadota, A., Suzuki, K., & Mori, K. (2001). Study on Flow Resistance Over Steep-Slope Gravel-Bed. *PROCEEDINGS OF HYDRAULIC ENGINEERING*, *45*, 619-624.

Konsoer, K. M., Rhoads, B. L., Langendoen, E. J., Best, J. L., Ursic, M. E., Abad, J. D., & Garcia, M. H. (2016). Spatial variability in bank resistance to erosion on a large meandering, mixed bedrock-alluvial river. *Geomorphology*, *252*, 80-97.

Lamarre, H., MacVicar, B., & Roy, A. G. (2005). Using passive integrated transponder (PIT) tags to investigate sediment transport in gravel-bed rivers. *Journal of Sedimentary Research*, *75*(4), 736-741.

Laronne, J. B., & Reid, L. (1993). Very high rates of bedload sediment transport by ephemeral desert rivers. *Nature*, *366*(6451), 148-150.

Marquis, G. A., & Roy, A. G. (2013). From macroturbulent flow structures to large-scale flow pulsations in gravel-bed rivers. *Coherent flow structures at Earth's surface*, 261-274.

Mosselman, E. (2012). Modelling sediment transport and morphodynamics of gravel-bed rivers. *Gravel-bed rivers: processes, tools, environments*, 101-115.

Mrokowska, M. M., & Rowiński, P. M. (2019). Impact of unsteady flow events on bedload transport: A review of laboratory experiments. *Water*, *11*(5), 907.

Palucis, M. C., Ulizio, T. P., Fuller, B., & Lamb, M. P. (2018). Flow resistance, sediment transport, and bedform development in a steep gravel-bedded river flume. *Geomorphology*, *320*, 111-126.

Papangelakis, E., & Hassan, M. A. (2016). The role of channel morphology on the mobility and dispersion of bed sediment in a small gravel-bed stream. *Earth Surface Processes and Landforms*, *41*(15), 2191-2206.

Parker, G., Fu, X., Lamb, M., & Venditti, J. (2020). Morphodynamics of downstream fining in rivers with unimodal sand-gravel feed.

Pfeiffer, A. M., Finnegan, N. J., & Willenbring, J. K. (2017). Sediment supply controls equilibrium channel geometry in gravel rivers. *Proceedings of the National Academy of Sciences*, *114*(13), 3346-3351.

Redolfi, M., Bertoldi, W., Tubino, M., & Welber, M. (2018). Bed load variability and morphology of gravel bed rivers subject to unsteady flow: A laboratory investigation. *Water Resources Research*, *54*(2), 842-862.

Robert, A. (2014). *River processes: an introduction to fluvial dynamics*. Routledge.

Roushangar, K., & Shahnazi, S. (2020). Prediction of sediment transport rates in gravel-bed rivers using Gaussian process regression. *Journal of hydroinformatics*, *22*(2), 249-262.

Singh, M., Singh, I. B., & Müller, G. (2007). Sediment characteristics and transportation dynamics of the Ganga River. *Geomorphology*, *86*(1-2), 144-175.

Wickert, A. D., & Schildgen, T. F. (2019). Long-profile evolution of transport-limited gravel-bed rivers. *Earth Surface Dynamics*, *7*(1), 17-43.

Wlodarczyk, K., Hassan, M. A., & Church, M. (2023). Annual and decadal net morphological displacement of a small gravel-bed channel. *Earth Surface Processes and Landforms*, *48*(8), 1630-1645.

Zhu, L. L., & Ge, H. (2014). Balance Adjustment of the gravel-sand river downstream reservoir. *Applied Mechanics and Materials*, *444*, 1218-1221.